Journal of Applied Polymer Science

Mechanical and Chemical Stability of Injection-Molded Microcantilevers Used for Sensing

Prabitha Urwyler,[1,2] Alfons Pascual,[3] Per Magnus Kristiansen,[3,4] Jens Gobrecht,[1,4] Bert Müller,[2] Helmut Schift[1,4]

[1]Paul Scherrer Institut, Laboratory for Micro- and Nanotechnology, 5232 Villigen PSI, Switzerland
[2]University of Basel, Biomaterials Science Center, c/o University Hospital, 4031 Basel, Switzerland
[3]University of Applied Sciences and Arts Northwestern Switzerland FHNW, Institute of Polymer Engineering, 5210 Windisch, Switzerland
[4]University of Applied Sciences and Arts Northwestern Switzerland FHNW, Institute of Polymer Nanotechnology, 5210 Windisch, Switzerland

Correspondence to: H. Schift (E-mail: helmut.schift@psi.ch)

ABSTRACT: Ultraviolet-ozone treatment is used as a standard surface cleaning procedure for removal of molecular organic contamination from analytical and sensing devices. Here, it is applied for injection-molded polymer microcantilevers before characterization and sensing experiments. This article examines the effects of the surface cleaning process using commercial equipment, in particular on the performance and mechanical properties of the cantilevers. It can be shown that the first chemical aging process essentially consist of the cross linking of the polymer chains together with a physical aging of the material. For longer exposure, the expected thermo-oxidative formation of carbonyl groups sets in and an exposure dependent chemical degradation can be detected. A process time of 20 min was found suitable as a trade-off between cleaning and stability. © 2012 Wiley Periodicals, Inc. J. Appl. Polym. Sci. 127: 2363–2370, 2013

KEYWORDS: microcantilever; polymer; injection molding; ultraviolet; ozone; degradation; polypropylene

Received 23 December 2011; accepted 15 March 2012; published online 9 May 2012
DOI: 10.1002/app.37767

INTRODUCTION

Disposable lab ware is essential in contemporary laboratory life. It is cost effective and meets the hygiene criteria. such as low microbiological contamination and ease of sterilization. Today, polystyrene (PS) and polypropylene (PP) are the most common polymers for such lab ware.[1] Recently, polymers have successfully entered the area of bioanalytics and -sensing. Mass production processes, including injection molding, have increasingly been used to manufacture products with microscopic dimensions, such as microfluidic platforms and diffractive optical elements.[2,3]

Microcantilevers (μCs), similar to those used in scanning force microscopy (SFM), have become popular as transducers in chemical and biological sensors.[4] In general, silicon technology was applied to produce these μC arrays. Due to growing interests in disposable devices in the life science sector, several manufacturing processes, including microinjection molding (μIM), have been developed to replace the rather expensive Si elements with polymeric ones.[3,5–9] Polymer materials offer tailored physical and chemical properties combined with low-cost mass production. Various polymers have been used to manufacture μCs using μIM. To ensure that polymeric μCs can be successfully applied under identical conditions, it has to be confirmed that the necessary cleaning procedures do not impair the μC's characteristics.

Cantilevers sense surface stresses transducing them into a bending, which is readily detected by laser deflection as in SFM systems. Surface selectivity toward biomolecules of interest is achieved by functionalizing cantilevers on one surface by immobilization of functional reagents (receptors). μCs are often gold coated to take advantage of thiol chemistry. Such thin gold films are also deposited on one side of the cantilevers to provide the necessary reflectivity for optical read-out.

A well-defined, homogeneously cleaned surface is a prerequisite for reproducible μC sensing. Organic contaminants not only impair receptor immobilization on cantilever surfaces but also affect the signal response of μCs and thus have to be removed according to suitable cleaning protocols. Plasma and ultraviolet-

© 2012 Wiley Periodicals, Inc.

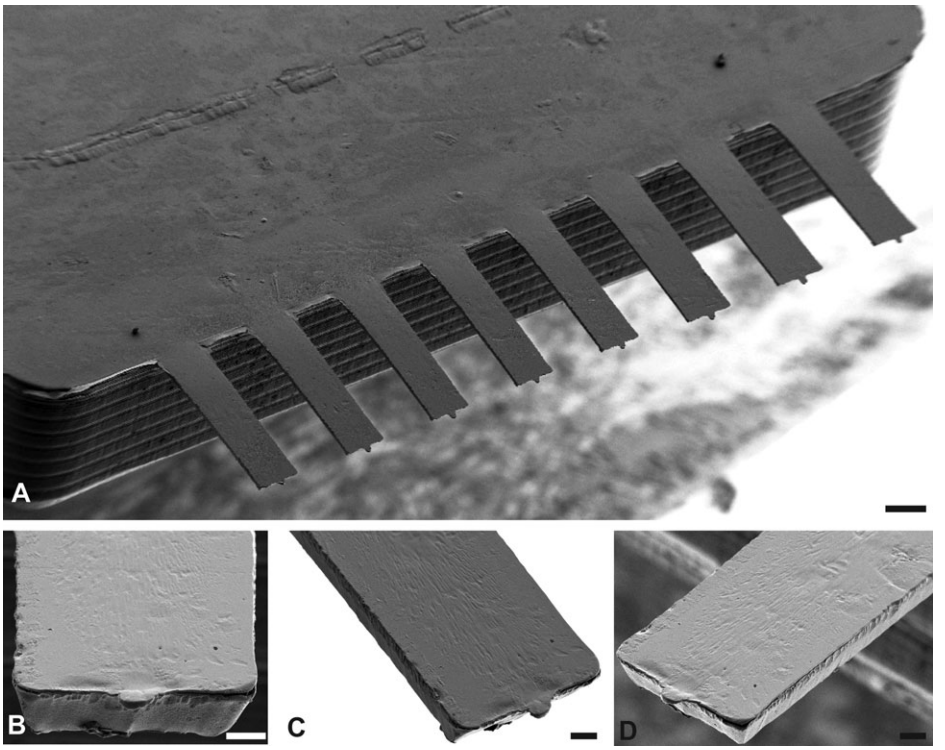

Figure 1. SEM micrograph of injection-molded PP μC with dimensions of 480 μm length, 80–130 μm width, and 30–36 μm thickness, showing outlines of the μC and part of the holder. The injection takes place from the holder into the cantilevers. Scale bar (A) 100 μm and (B–D) 20 μm.

ozone (UVO) treatments belong to the common dry cleaning procedures. In such plasma cleaning, the contaminants are removed using a combination of chemical reactions and physical, ballistic impact of gas molecules. Despite the straightforward application of plasma treatment, the availability of required vacuum systems limits the use in numerous laboratories. UVO treatment can be carried out at ambient conditions and, can thus be applied nearly everywhere. The mechanism behind UVO cleaning is a photosensitized oxidation process in which the contaminant molecules are dissociated by the absorption of UV light.[10] In addition, UV light converts atmospheric oxygen into reactive ozone. Ozone attacks the smaller fragments and thereby creates volatile organics, which desorb from the surface.[10] Consequently, UVO cleaning effectively removes the organic contaminants. Commercially available silicon μCs are regularly cleaned taking advantage of an UVO treatment for a period of 50 min.[11]

The surface of polymeric μCs, however, is also attacked by the UVO treatment, a process that may lead to undesired degradation. The rate of polymer degradation depends on the chemical composition. The latter not only determines the susceptibility to damage by incident irradiation (spectral sensitivity) but also paths of thermo-oxidative degradation and reactivity toward aggressive media, such as ozone and other atmospheric pollutants.[12] The combined impact of UV irradiation and oxygen generally causes chain scission reducing the mechanical and surface properties of the polymers, which could finally lead to device failure. Furthermore, the glass transition temperature of UVO-treated polymers is severely changed.[13]

The morphology of the injection-molded polymeric μCs strongly influences the sensitivity to degradation and deformation potential. Particularly, the amorphous skin layer which results from rapid cooling on contact with the mold is more prone to degradation than the bulk of the cantilever.[14] These factors determine whether the organic contaminants can be removed from polymeric μC surfaces before degradation and concomitant deterioration of the mechanical properties occurs. Hence, there is the need to investigate the effects of UVO treatment on polymeric cantilevers bearing in mind the need for a compromise between surface decontamination and cantilever maintenance. This is done through identification of appropriate treatments and exposure times to which injection-molded polymeric μCs could be subjected.

EXPERIMENTAL

Cantilever Manufacture

Polymeric μCs were produced using a modular injection molding tool as described previously.[8,9] The molding tool is installed in an Arburg 320 Allrounder (Arburg, Lossburg, Germany) with a maximum clamping force of 600 kN. The mirror unit of the molding tool, a polished steel surface ensured an optically flat and smooth surface. The μC array was designed with outlines of a micromachined 500 μm-thick silicon μC array with a 3.5 mm $\times$ 2.5 mm large body (holder). It has eight 480 μm long and 80–130 μm-wide μC beams as shown in Figure 1(A). The μC mold cavity depth was in the range between 30 and 36 μm. Due to the laser ablation process, the cross section of the μC is trapezoidal as shown in Figure 1(B). The width of the

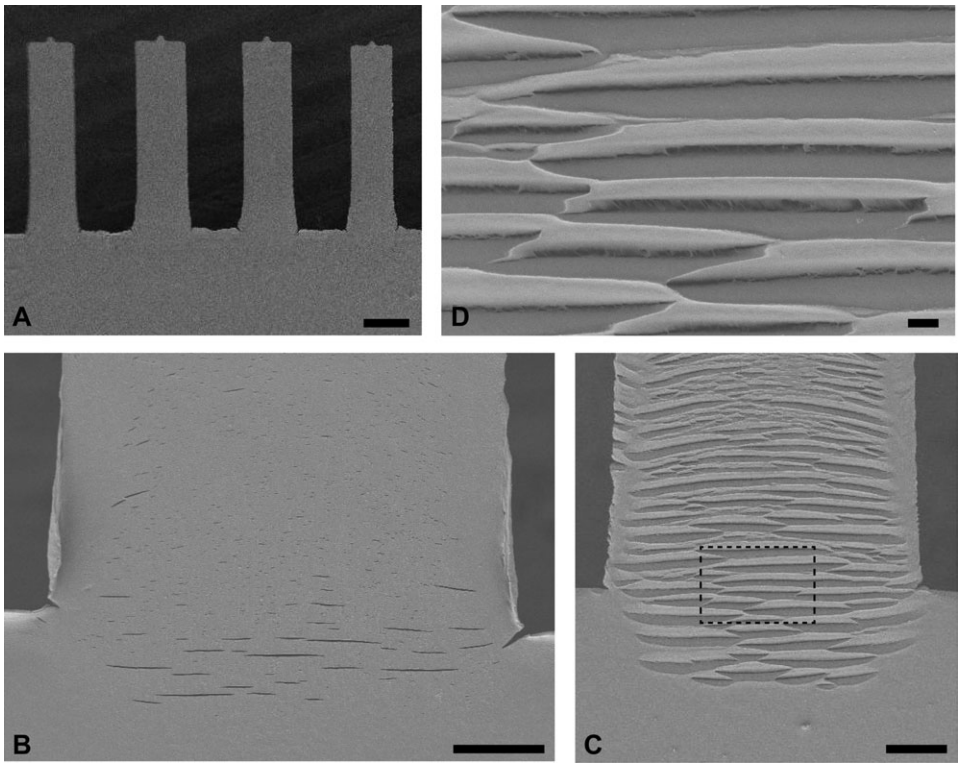

Figure 2. SEM observation of surface damage evolution with the UVO exposure: (A) 30 min, (B) 60 min, (C) 120 min, and (D) close-up of the surface cracks developed after 120 min. Scale bar (A) 100 μm, (B and C) 20 μm, and (D) 2 μm.

cantilevers is about 20 μm smaller on the laser-ablated bottom than on the mirror side of the molding tool. The injection molding process parameters were melt temperature 200°C, tool temperature 40°C, and injection speed 9 cm^3 s^{-1}, i.e. similar to those used previously.[8,9]

Polymer Materials

Metallocene polypropylene (m-PP: Metocene HM 648T, LyondellBasell, Germany) was used as model polymer due to its pronounced shear thinning that favors filling of microcavities in injection molding applications. Other polymers used in the bioanalytical devices. such as cyclic olefin copolymer (COC: Topas 8007x10), polyoxymethylene (POM-C: 511P Delrin NC010), and polyvinylidenfluoride (PVDF: Kynar 720 Arkema) were also molded with the tool but not investigated in detail. However, because of the superior mold filling of PP and their subsequent application in sensing applications, the detailed investigation of the UVO exposure was conducted using the molded PP μCs only. Injection-molded PP μCs were stored at ambient conditions for at least 1 week before use to allow postcrystallization as the molded product's mechanical characteristics change substantially within the first 24 h after molding.[15]

Cantilever Finishing

Physical vapor deposition coating of cantilevers was carried out with a laboratory thermal evaporator (Balzers BAE 250, Balzers, Liechtenstein) employing evaporation material from Umicore (Cr and Au, both 99.99%). The layer thickness was controlled by means of a quartz crystal microbalance integrated in the evaporation system. PP μCs were first coated on the flat mirror side with a 4-nm thin chromium film as adhesion promoter for the subsequently deposited 20-nm thin gold layer, which guaranteed sufficient laser beam reflectivity for use in the Cantisens® research system (Concentris GmbH, Basel, Switzerland) for measuring deflection.

Cantilever Surface Cleaning

The flat mirror side of the cantilever surface was treated in a UVO cleaner (UV Clean Model 13550, Boekel Scientific, Feasterville PA). Batches of gold-coated and bare μCs were cleaned for periods ranging from 2 to 120 min. Cleaning experiments of other polymeric μCs (PVDF, POM, and COC) were also conducted.

Cantilever Characterization

Surface inspection was carried out by means of optical microscopy (DMRX, Leica Microsystems Jena GmbH, Germany) and scanning electron microscopy (SEM: Supra 55 VP, Carl Zeiss NTS GmbH, Oberkochen, Germany).

Reflection Fourier transform infrared (FTIR) spectra of two regions on the μC array, i.e. close to the cantilever fingers and holder, respectively, were recorded using a Centaurus IR-microscope coupled to a Nexus IR spectrometer (Thermo Electron, Thermo Fisher Scientific, Dreieich, Germany) with a grid of 300 μm × 300 μm. Two μC arrays of non-UVO-treated specimens were measured as reference. The background spectra were recorded every 15 min.

For the thermal analysis, the μC arrays with a mass between 3 and 4 mg were sealed to an aluminum cup to acquire

Applied Polymer SCIENCE

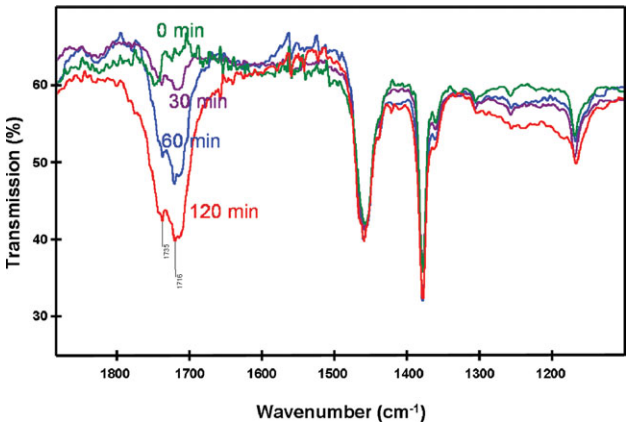

Figure 3. FTIR-Spectrum (reflection) of a PP μC in the region between 1850 and 1100 cm^{-1}. Two partially overlapping signals (1715 and 1735 cm^{-1}) show the formation of carbonyl and ester groups, their intensity correlating with the UVO exposure time. [Color figure can be viewed in the online issue, which is available at wileyonlinelibrary.com.]

differential scanning calorimeter (DSC: DSCQ1000, TA Instruments, Waters GmbH, Eschborn, Germany) data. The complete protocol, consisting of a first heating cycle from 0°C to 250°C, subsequent cooling to 0°C and a second heating cycle again to 250°C, was conducted in a dry nitrogen atmosphere. The heating and cooling rates were set to 10 K min^{-1}.

To evaluate the thermal behavior (bimetallic test), the gold-coated PP μCs were introduced into the water-filled cell of the Cantisens® research system maintained at 25°C. The temperature was increased at a rate of 0.2 K s^{-1} from 25°C to 30°C, and the bending response of each μC was recorded. The cantilevers bend because of the different thermal expansions of polymer and metal. The series of heat tests followed by an UVO exposure was conducted using three PP μC arrays from a single batch.

To determine the μC's hardness, the PP μCs were mounted on aluminum stubs by means of carbon tape for indentation tests. The hardness and elastic modulus of the μCs exposed to UVO were determined using a nanoindenter (MTS XP®, MTS Systems, Cary, NC) with a 1 μm conical tip (XP/CON100/001). For practical reasons, the indentation measurements were carried on the array holder and not on the μC itself. Indentations at two locations of each array were averaged. A maximum load of 5 mN was applied using a loading rate of 0.1 mN s^{-1}. The holding time was set to 30 s at maximum load, which allows the material to relax and clears the unloading data set from the creeping phenomena. The Poisson's ratio of PP corresponds to 0.4, as given by the supplier (see datasheet).

Bending tests were performed using a nanoindentation system (MTS XP®) operated under the load-control mode. A flat punch probe (XP/FLT 090/D0050) placed at the center of the UVO-treated PP μC was used to apply a load of 1 mN at maximum. The loading rate corresponded to 0.066 mN/s. The holding time was again set to 30 s.

RESULTS AND DISCUSSION

Materials Selection and μC Cross Section

Of the polymers tested, m-PP was most suitable for preparation of μCs as its pronounced shear thinning at relatively low temperatures enabled ready filling of the mold cavities. Figure 1 shows an SEM micrograph of injection-molded PP μCs. The μCs exhibit a trapezoid cross section [see Figure 1(B)], which reflects a relatively large draft angle compared with standard injection molding products. This draft angle facilitates demolding of the rather thin μC beams avoiding undesired plastic deformation.

Cantilever Characterization

The UVO cleaning procedure removes molecular levels of non-intentionally adsorbed organic species (contaminations) yielding a clean cantilever surface. Because the 20-nm thin gold coating does not present a major optical barrier for the UV light, the analysis is usually related to bare μCs. Mechanical degradation effects were expected to be equal or larger for the bare than for the gold-coated μCs.

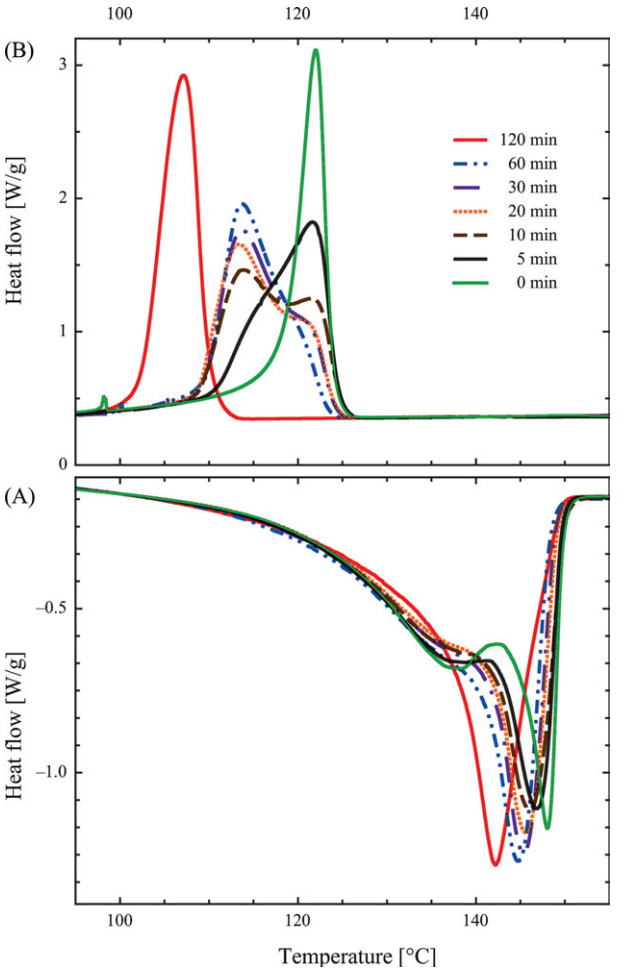

Figure 4. DSC measurement of PP μC arrays for different UVO exposure times displaying changes in the melting (A) and crystallization (B) behavior. [Color figure can be viewed in the online issue, which is available at wileyonlinelibrary.com.]

Table I. Summary of the Results From DSC Analysis of PP μCs Exposed to Different Doses of UVO

UV-ozone exposure (min)	0	2	5	10	15	20	30	60	120
1st heating									
T_{g1} (°C)	53	53	52	56	57	60	49	49	48
T_{m1} (°C)	146	146	146	146	146	146	147[a]	92/144	104/143
ΔH_{m1} (J/g)	72	76	78	78	78	75[b]	84	88	86
Cooling									
T_c (°C)	122	122	122	121/114	114[a]	113[a]	114	114	107
ΔH_c (J/g)	91	92	93	93	93	91[a]	92	94	89
2nd heating									
T_{m2} (°C)	139/148	138/148	139/147	145[a]	146[a]	146[a]	145	145	142
ΔH_{m2} (J/g)	93	95	95	94	94	93[b]	95	97	94

[a]Shoulder, [b]Actual numerical values of the enthalpies may be slightly higher than shown.

Figure 2, which is composed of SEM micrographs of a PP μC array after UVO treatment for different durations of exposure, shows significant morphological changes for exposure times above 30 min. For exposure times longer than 30 min, both optical microscopy and SEM [cp. images in Figure 2(B–D)] revealed crack-like microstructures on the μCs associated with surface etching, a phenomenon also present for the gold-coated μCs. This means that the coating does not prevent UVO etching of PP μCs for exposure times above 30 min.

SEM data show that the surface roughness increases with exposure time, as observed for oxygen plasma treatments.[16] Two kinds of surface patterns were distinguishable, one of flow lines and the other of microcracks. Flow lines correspond to surface textures or voids owing to local filling inhomogenities along the flow direction. The microcracks are formed almost perpendicular to the μC direction illustrating flow instabilities caused during filling of the micrometer-thin mold cavity. The microcracks, which are discontinuous along the μC, are first formed at the base of the μCs. With increasing UVO exposure time, they evolve like bands along the entire μC. The microcracks are almost straight at the base of the μC and later follow the polymer flow direction along the length of the μC. They seem to be the result of polymer shrinkage in the beam direction. This may arise from the nonlinear flow front owing to the lower viscosity at the sidewalls of the mold.

On UVO exposure the polymer degrades. This means that due to the transparency of PP to UV light, low molecular weight fragments are formed through chain scission in the entire holder, resulting in a reduced glass transition temperature T_g.[17,18] They undergo oxidative reactions, once cracks are formed at the surface. Callen et al.[19] demonstrated that UVO treatments of PS produces oxidized polymer surfaces comprising of C—O, C=O, and O—C=O groups.

The FTIR spectra of the UVO-exposed PP μCs, as shown in Figure 3, feature two carbonyl signals at the wavelengths of 1734 cm^{-1} (ester) and 1716 cm^{-1} (ketone or unsaturated ester), indicating thermo-oxidative aging. Comparing the spectra for the selected exposure times, a detection threshold for the carbonyl bands of about 20 min can be identified. For longer exposure times, the carbonyl-related peak intensities correlated well with the duration of the UVO treatment. Carboxylic acids and free OH groups are present at wavelengths of about 3400 cm^{-1} (intermolecular OH bonds; not shown in Figure 3). These signals became stronger for exposure times of 60 and 120 min.

Complementary information regarding the underlying physical and chemical phenomena was gained through thermal analysis by means of DSC. For this purpose μCs with UVO treatments were subjected to heating and cooling cycles. Figure 4 and Table I summarize the transition temperatures and enthalpies. Increasing the exposure time, the transition temperatures shifted to smaller values. The degree of crystallinity, characterized by means of ΔH_{m1}, increases with the exposure time. An UVO exposure less than 30 min leads to an increase in crystallinity of 5–10%, whereas an exposure of 30 min and longer increases the crystallinity up to 25%. Such significant changes in crystallinity are characteristic for physical aging in semicrystalline polymers.[20] The cooling reveals that the recrystallization is shifted

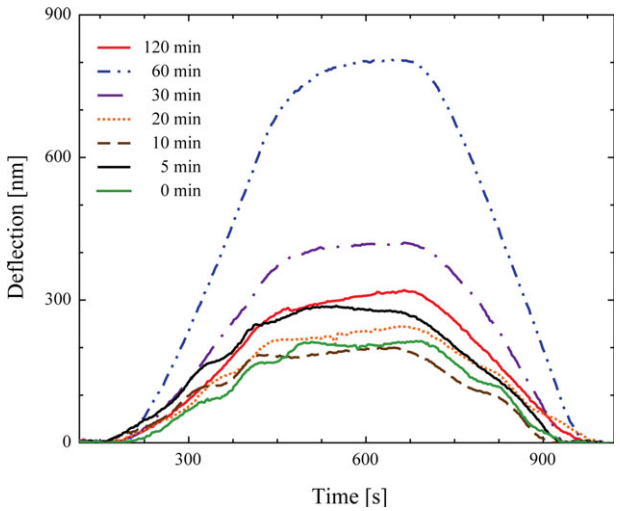

Figure 5. Deflection due to the bimetallic effect of the gold-coated PP μC #5 for the different UVO exposure times. [Color figure can be viewed in the online issue, which is available at wileyonlinelibrary.com.]

Applied Polymer SCIENCE

Table II. Maximum Deflection Recorded During the Heat Test of the Gold-Coated UVO-Exposed PP μCs (Results Averaged for All eight μCs From three Samples)

UV-ozone exposure (min)	0	2	5	10	15	20	30	60	120
Deflection (nm)									
μC array 1	270 ± 139	264 ± 110	292 ± 122	168 ± 130	213 ± 92	344 ± 153	686 ± 175	602 ± 347	483 ± 120
μC array 2	196 ± 91	298 ± 98	249 ± 80	279 ± 133	202 ± 73	208 ± 80	384 ± 182	526 ± 77	288 ± 147
μC array 3	267 ± 187	374 ± 174	273 ± 190	428 ± 254	295 ± 164	383 ± 218	458 ± 179	446 ± 196	352 ± 168

Table III. Deformation Characteristics of the Surface of the UVO Exposed PP μC Array Holders as Determined From Indentation Experiments

UV-ozone exposure (min)	0	2	5	10	15	20	30	60	120
Modulus (MPa)	887 ± 18	783 ± 28	632 ± 17	242 ± 60	808 ± 37	1060 ± 70	1001 ± 2	1314 ± 67	1467 ± 28
Hardness (MPa)	21 ± 0.42	17 ± 1	16 ± 0.32	1 ± 0.2	19 ± 1	26 ± 1	20 ±1	22 ± 0.44	18 ± 0.36

toward smaller transition temperatures, an effect already detected for exposure times as small as 5 min. The related enthalpy ΔH_c, however, is unaffected for exposures up to 20 min. This behavior indicates the onset of *cross linking*. A decreasing melting temperature (T_m) with increasing exposure time is observed for the second heating cycle shown in Figure 4. This effect is attributed to *chemical aging* initiated already after an UVO exposure of 5 min. Additionally, the appearance of a secondary peak at the temperature T_{m1} during the melting process is only observed for exposure times of 30, 60, and 120 min. The glass transition temperature T_g amounts to 56 ± 4°C for UVO exposures up to 20 min (see Table I). Longer exposures result in a drop by about 10 K.

The mechanical behavior of gold-coated, UVO-treated μCs was characterized taking advantage of the thermally induced bending of the biphasic cantilever, often referred to as heat test.[21] Due to the difference in the linear coefficient of thermal expansion (α) of the 24-nm thin metal ($\alpha_{gold} = 14.2 \times 10^{-6}$ K^{-1}) and the 35-μm thick PP ($\alpha_{PP} = 150 \times 10^{-6}$ K^{-1}), the μC bends, which is detected through laser beam deflection at the μC free end. Figure 5 shows deflection curves of selected PP μCs after UVO treatment. For exposure times up to 20 min, the curves illustrate some variations but are comparable to the base line (no UVO treatment). The increase in the deflection signal for 30 and 60 min exposures coincidences with the observation of crack-like surface microstructures in optical microscopy. The variation in the mean deflection values as given in Table II, demonstrates that the deflection can massively change from array to array. The main result, a step-like increase in the deflection signal between 20 and 30 min of exposure time, leads to the conclusion that the μCs can be UVO treated for up to 20 min.

Nanoindentation usually provides mechanical data of a combination of surface and bulk properties and might, thus, be more appropriate to characterize the UVO-induced modifications of the

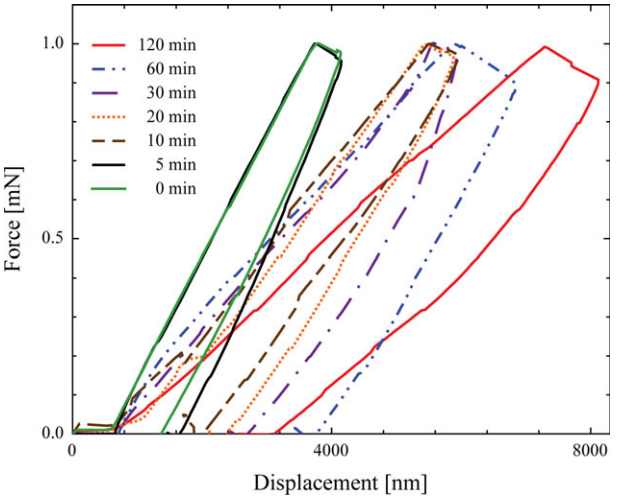

Figure 6. Load–deflection curves from the bending of the PP μC using the nanoindenter. The Young's modulus of the PP μC was obtained from the slope of the load–deflection curve (cf. Table IV). [Color figure can be viewed in the online issue, which is available at wileyonlinelibrary.com.]

Table IV. Deformation Characteristics of UVO-Exposed PP μCs as Determined From Bending Experiments

UV-ozone exposure (min)	0	2	5	10	15	20	30	60	120
Modulus (GPa) (eq. (1))	3.16 ± 0.44	2.78 ± 0.83	3.07 ± 0.64	2.07 ± 0.96	2.16 ± 0.94	2.71 ± 0.39	2.76 ± 0.15	1.62 ± 0.39	1.40 ± 0.35
Stiffness (N/m)	241 ± 26	216 ± 65	209 ± 65	161 ± 75	168 ± 17	210 ± 29	214 ± 38	126 ± 29	108 ± 27

μCs. Such a measurement does not only allow for determination of the local hardness but also of the Young's modulus from the slope of the unloading curve.[22] Table III summarizes these two quantities, including their error bars as a function of exposure time. After a decrease during the first 10 min of exposure, the Young's modulus increases with exposure time but a pronounced, distinct change between 20 and 30 min UVO treatments cannot be found. On the contrary, the hardness shows a maximum for 20 min exposure. Nevertheless we assume that the hardness is largely insensitive to UVO treatments, which may arise from the fact that not the cantilevers themselves but the rather bulky connection part of the cantilever array was tested, where no or few cracks are formed at extended UVO exposure times.

Figure 6 displays load–displacement curves (P–z) of PP μC as a function of UVO exposure time. The elastic modulus of the μC can be derived using the equation:

$$E = \frac{4L_e^3}{wt^3}\left(\frac{P}{z}\right) \quad (1)$$

where w and t denote the μC width and thickness, respectively. L_e is the equivalent beam length between the loading position and the fixed end of the μC. The parameter (P/z) is the stiffness of the μC associated with the length L_e, and is given by the slope of the load–displacement curve. Table IV summarizes the mean values, including error bars. For UVO exposure times of up to 30 min, both Young's modulus and stiffness remain constant. Both experimental values significantly decline for UVO treatments above 30 min. Therefore, we conclude from the bending measurements that exposure times larger than 30 min have to be avoided to maintain the desired bending characteristics.

CONCLUSIONS

UVO treatment can significantly influence the physical and chemical properties of PP μCs. A reasonable compromise between the negative impact on the latter and the cleaning efficacy was found for UVO exposure times up to 20 min. Longer UVO treatments cannot be tolerated as severe deterioration of the bending and surface characteristics takes place. Nanometer-thin gold coatings, often deposited to obtain reasonable laser beam reflectivity, do not prevent the μC degradation but cause a moderate retardation of the UVO-induced property modification.

ACKNOWLEDGMENTS

This research was funded by the Swiss Nanoscience Institute (SNI) through the applied research project DICANS, a collaborative initiative between the Biomaterials Science Center (BMC) of the University of Basel, the Paul Scherrer Institut (PSI), the University of Applied Sciences Northwestern Switzerland (FHNW) and Concentris GmbH. The authors thank K. Jefimovs (EMPA Dübendorf) for the laser micromachining of the mold, O. Häfeli and E. Kramer (FHNW Windisch) for the injection molding and polymer analysis, R. Ghisleni (EMPA Thun) for his assistance with the MTS XP® system, M. Altana and C. Spreu from PSI for their technical assistance.

REFERENCES

1. Greiner bio-one. Chemical-and-thermal-resistance-of-polypropylene–polystyrene–LDPE–HDPE–EVA and UV-Star. http://www.biocompare.com/Articles/ApplicationNote/1609/
2. Giboz, J.; Copponnex, T.; Mélé, P. *J. Micromech. Microeng.* **2007,** *17*, 96–109.
3. Heckele, M.; Schomburg, W. K. *J. Micromech. Microeng.* **2004,** *14*, R1–R14.
4. Berger, R.; Gerber, C.; Lang, H. P.; Gimzewski, J. K. *Microelectron. Eng.* **1997,** *35*, 373–379.
5. Genolet, G.; Despont, M.; Vettiger, P.; Anselmetti, D. *J. Vac. Sci. Technol. B* **2000,** *18*, 617–620.
6. Nordström, M.; Keller, S.; Lillemose, M.; Johansson, A.; Dohn, S.; Haefliger, D.; Blagoi, S.; Havsteen-Jakobsen, S.; Boisen, A. *Sensors* **2008,** *8*, 1595–1612.
7. McFarland, A.; Poggi, M. A.; Bottomley, L. A.; Colton, J. S. *Nanotechnology* **2004,** *15*, 1628–1632.
8. Urwyler, P.; Schift, H.; Gobrecht, J.; Häfeli, O.; Altana, M.; Battiston, F.; Müller, B. *Sens. Actuators A: Phys.* **2011,** *172*, 2–8.
9. Urwyler, P.; Häfeli, O.; Schift, H.; Gobrecht, J.; Battiston, F.; Müller, B. *Procedia Eng.* **2010,** *5*, 347–350.
10. Vig, J. R. *J. Vac. Sci. Technol. A* **1985,** *3*, 1027–1034.
11. Köser, J.; Gaiser, S.; Müller, B. *Eur. Cells Mater.* **2011,** *21*, 479–487.
12. Wypyh, G. Handbook of Material Weathering; ChemTec Publishing: Toronto, **2003.**
13. Bhattacharyya, A.; Klapperich, C. *Lab Chip* **2007,** *7*, 876–882.
14. Zhou, Q.; Xanthos, M. *Polym. Degrad. Stabil.* **2009,** *94*, 327–338.
15. Kristiansen, M.; Tervoot, T.; Smith, P.; Goosens, J. P. G. *Macromolecules* **2005,** *38*, 10461–10465.
16. Tsougeni, K.; Vourdas, N.; Tserepi, A.; Gogolides, E.; Cardinaud, C. *Langmuir* **2009,** *25*, 11748–11759.
17. Nie, H.-Y.; Walzak, M. J.; Berno, B.; McIntrye, N. S. *Appl. Surf. Sci.* **1999,**144–145,627–632.
18. Eve, S.; Mohr, J. *Procedia Eng.* **2009,** *1*, 237–240.
19. Callen, B. W.; Ridge, M. L.; Lahooti, S.; Neumann, A. W.; Sodhi, R. N. S. *J. Vac. Sci. Technol. B* **1995,** *13*, 2023–2029.
20. Msuya, W. F.; Yue, C. Y. *J. Mater. Sci. Lett.* **1989,** *8*, 1266–1268.
21. Urwyler, P.; Köser, J.; Schift, H.; Gobrecht, J.; Müller, B. *Biointerphases* **2012,** *7*, 8.
22. Cheng, C.-M.; Cheng, Y.-T. *Appl. Phys. Lett.* **1997,** *71*, 2623–2625.